Magnetic behavior of probe layers of ^{57}Fe in thin Fe films observed by means of nuclear resonant scattering of synchrotron radiation

L. Niesen, A. Mugarza,* and M. F. Rosu
Nuclear Solid State Physics, Materials Science Centre, Groningen University, Nijenborgh 4, 9747 AG Groningen, The Netherlands

R. Coehoorn, R. M. Jungblut, and F. Roozeboom
Philips Research Laboratories, Box WA-14, 5656 AA Eindhoven, The Netherlands

A. Q. R. Baron,† A. I. Chumakov, and R. Rüffer
European Synchrotron Radiation Facility, BP 220, F-38043 Grenoble, France
(Received 4 November 1997)

The magnetic behavior of epitaxial probe layers of ^{57}Fe down to a thickness of 1 monolayer (ML) has been investigated with the technique of nuclear resonant scattering by synchrotron radiation (NRS) in a grazing-incidence geometry. The samples consisted of 10–55 ML Fe deposited onto a Ge(100) substrate and covered with 2 nm Au. Probe layers of 1–10 ML ^{57}Fe were inserted at different depths in the Fe film. The technique yields spectroscopic information, i.e., magnetic hyperfine fields and isomer shifts, as well as structural information, such as layer thicknesses and interface roughness. The results show the existence of a nonmagnetic Ge/Fe interlayer of at least 10 ML thick after deposition at room temperature. Subsequent conversion electron Mössbauer spectroscopy (CEMS) data show that, although the samples were stored at room temperature, the interlayer diffusion proceeds as a function of time. The relative merits of NRS and CEMS for the investigation of ultrathin layers are discussed. [S0163-1829(98)03137-3]

I. INTRODUCTION

Metallic multilayers in which one of the components is magnetic are currently a topic of much interest because they show interesting phenomena like ferromagnetic/antiferromagnetic coupling as a function of nonmagnetic spacer thickness, giant magnetoresistance and perpendicular anisotropy.[1] It has become clear that in many cases the magnetic behavior is intimately associated with the structure of the interfaces.[1] One of the key issues, therefore, is the description of interface magnetism in terms of different atomic sites at the interface.

Mössbauer spectroscopy on magnetic multilayers containing ^{57}Fe is a well known technique for the study of the magnetic behavior of these layers. Similar to the magnetic moment, the magnitude and direction of the observed magnetic hyperfine field is directly related to the local electronic structure of the Fe atoms. At the interface, where the local symmetry is broken, one can also observe the interaction between the quadrupole moment of the ^{57}Fe nucleus and the resulting electric field gradient (the quadrupole interaction). Because the magnetic hyperfine field is sensitive to the direct surroundings of the probe nucleus, this quantity can also give structural information. Interface roughness, for instance, can be studied by inserting the ^{57}Fe probes at different depths from the interfaces and measuring the resulting distribution of hyperfine fields. By detecting the conversion electrons emitted by the ^{57}Fe nucleus that absorbed the 14.4 keV photon one obtains a sensitivity of about 1 monolayer. The limit is determined by the nonresonant background. This CEMS technique has been applied for instance to the system Fe/Ag (100).[2,3]

The recent construction of a nuclear resonance beamline at the European Synchrotron Radiation Facility (ESRF) has opened up the possibility for observation of the hyperfine interaction of minute quantities of ^{57}Fe by nuclear resonant scattering in a grazing-incidence geometry.[4] Similar beam lines are completed, respectively under construction at the American Photon Source (APS) near Chicago and at the SPring8 facility near Hyogo, Japan. Earlier, this technique has already been applied successfully to the study of thicker (multi)layers.[5,6] A sample of ^{57}Fe nuclei is excited by a short (100 ps) pulse of synchrotron radiation. If a hyperfine interaction is present, the time evolution of the nuclear scattering shows a characteristic beat pattern, with frequencies corresponding to the energy level differences, superimposed on a decay with a characteristic time of the order of the lifetime of the nuclear level (141 ns). In contrast, the electronic response of the system (elastic scattering, photoeffect, Compton effect) is ''prompt'' on this time scale. Even though the electronic response is normally much stronger than the nuclear response, the latter can be observed with very low background in a suitable time window after the exciting pulse.[4] Provided one can obtain a sufficiently high counting rate, this method will be more sensitive than the CEMS technique. Another advantage is that one can easily study the hyperfine interaction as a function of temperature and/or external magnetic field. Finally, because the beam is nearly 100% polarized in the horizontal plane, one obtains more detailed information about the directional distribution of the magnetic moments in the sample.

In order to test the possibilities of this technique for the study of thin layer magnetism, we have chosen the system Fe/Au(001), which can be grown epitaxially with good quality on a Ge substrate.[7,8] The results show that it is possible to measure the signal of one monolayer of ^{57}Fe. Contrary to CEMS, the sensitivity limit is determined by counting rate rather than background. Although in particular Anderson

et al.[8] claim a sharp interface between the *S*-passivated Ge substrate and the Fe overlayer, our results demonstrate a considerable interdiffusion, which proceeds as a function of time.

II. EXPERIMENT

Samples were prepared in the metal-MBE set up at Philips Research Laboratories in Eindhoven. Three samples were grown on a Ge(001) substrate of 0.3 mm thickness and dimensions 18×14 mm^2. The substrate preparation was done in the same way as in Ref. 8. Prior to introduction in the UHV chamber the substrate was rinsed with HF and treated with $(NH_4)_2S$ for 20 min at 70 °C. This leads to the formation of a *S*-passivated surface layer.[8,9] The substrates were annealed at 190 °C for 2 h in UHV before deposition. Samples *A* and *B* consisted of 40 monolayers (ML, 1 ML$=$0.143 nm) natural Fe grown on the Ge substrate, followed by 10 ML of ^{57}Fe and another 5 ML of natural Fe. Thicknesses were measured by means of a quartz crystal microbalance. LEED experiments performed right after growth showed a good quality Fe(100) pattern. These and all other samples were covered with $\approx$2 nm Au to prevent oxidation and to provide a well defined interface. For these samples we use the notation Ge/40Fe/10^{57}Fe/5Fe/Au. The composition of sample *C* was Ge/5Fe/4^{57}Fe/2Fe/Au. Two other samples were grown on a 6 mm thick, non *S*-passivated Ge substrate with dimensions 20×45 mm^2, sputter-cleaned *in situ* for 45 min at 700 °C and annealed for 2 h at 780 °C. Compositions were for sample *D*: Ge/10Fe/1^{57}Fe/4Fe/Au and for sample *E*: Ge/14Fe/1^{57}Fe/Au. Sample *A* was grown at 200 °C, all other samples at room temperature. Right after they were taken out of the MBE set up, the overall magnetic behavior of the first three samples was studied by the magneto-optical Kerr effect (MOKE). Soft ferromagnetic behavior was observed in all cases when the samples were magnetized in the [100] easy direction. The magnetization reached saturation already in a field of $\approx$3 mT.

Nuclear resonance scattering was performed at beamline ID 18 of the ESRF, with the storage ring running in a mode with 16 bunches, 176 ns apart. The beam from the undulator was monochromatized in two steps to a bandwidth of 6 meV around the 14413 eV resonance in ^{57}Fe. Typical dimensions of the photon beam were 0.3 mm vertical and 1.5 mm horizontal. The sample plane was nearly horizontal, with the longest sample dimension (100) making a small, adjustable angle Θ with the beam. The scattering plane was vertical and the scattering angle of 2Θ was defined by slits in front of the sample and the detector. The scattered photons were detected in a 10×10 mm^2 avalanche photodiode (EG&G),[10] located $\approx$30 cm downstream from the sample. In order to align the magnetization perpendicular to the beam, a magnetic field of 15 or 44 mT was applied along the horizontal (010) axis, parallel to the linear polarization of the incoming photon beam. Typically, 10^8 prompt photons/s were collected (i.e., 10–20 photons per pulse), while we registered at most 10 s^{-1} delayed events from the nuclear resonant scattering process. Due to the fast time response of the avalanche photodiode (APD) the delayed counts could be observed without interference from the prompt response in an interval 20–160 ns after the exciting photon pulse. The background of the APD was very low (0.01–0.02 s^{-1}). Time spectra were obtained using standard fast time electronics.[4]

III. THEORETICAL DESCRIPTION OF NUCLEAR RESONANCE SCATTERING IN GRAZING INCIDENCE

In a nuclear resonance scattering experiment the sample is excited by a photon pulse which is so short that its frequency spectrum is much broader than the typical hyperfine interaction spectrum associated with the splitting of the ground and excited nuclear state. Whereas the response of the electrons is prompt, the nuclear time response is basically governed by the lifetime of the excited state. The response displays a characteristic beat pattern if the nuclear levels are split by the hyperfine interaction, but it depends also on the geometric arrangement of the scatterers and on the incidence angle. This is described by the dynamical theory of nuclear resonance scattering.[11,12] In this theory, the nuclear resonant layer is described by a frequency-dependent complex refractive index $n=1-\delta$, where δ is proportional to the number density of recoilless resonant scatterers and to the nuclear scattering amplitude of an individual ^{57}Fe nucleus. The latter quantity is a sum of complex Lorentzians describing the individual transitions. The relative amplitudes of these Lorentzians depend on the the polarization state of the photons and on the orientation of the photon wave vector $\mathbf{k}$ with respect to the quantization axis used to describe the hyperfine interaction. The total frequency dependent reflectivity of the multilayer, $R(\omega)$, is calculated by applying the Fresnel coefficients for reflection and transmission at each interface, taking into account the propagation through the layers. Interface roughness is included in the Nevot-Croce approximation.[13] In principle this calculation must be performed for two independent components of the polarization vector. However, for the case of ^{57}Fe and the geometry used in the present experiment (quantization axis perpendicular to the beam direction and parallel to the linear polarization vector) we have only one relevant polarization component. In this case the nuclear scattering amplitude is the sum of the four complex Lorentzians describing the $\Delta m=\pm1$ transitions between the sublevels of the $I=1/2$ ground state and the $I=3/2$ excited state of the ^{57}Fe nuclei. After a pulse excitation, the time dependence of the amplitude of the wave scattered in the forward direction, $G(t>0)$, is given by

$$G(t>0)=(2\pi)^{-1}\int_{-\infty}^{\infty}[R(\omega)-R_e(\omega)]e^{i\omega i}\,d\omega, \qquad (1)$$

where $R(\omega)$ is the total reflectivity including the nuclear scattering and $R_e(\omega)$ is the electronic reflectivity. The measured signal is proportional to $|G(t>0)|^2$.[14]

IV. EXPERIMENTAL RESULTS

$\Theta-2\Theta$ scans of both the prompt and the delayed reflected intensity were obtained for the thicker samples *A* and *B* by varying Θ in an interval 0–25 mrad and adjusting the height of the slit-detector combination. The result for sample *A* is displayed in Fig. 1. The prompt response [Fig. 1(a)], measured with a beam height of 25 μm, shows Kiessig beats[15] associated with interference between beams reflected from the back and front side of the Fe layer. The solid line is

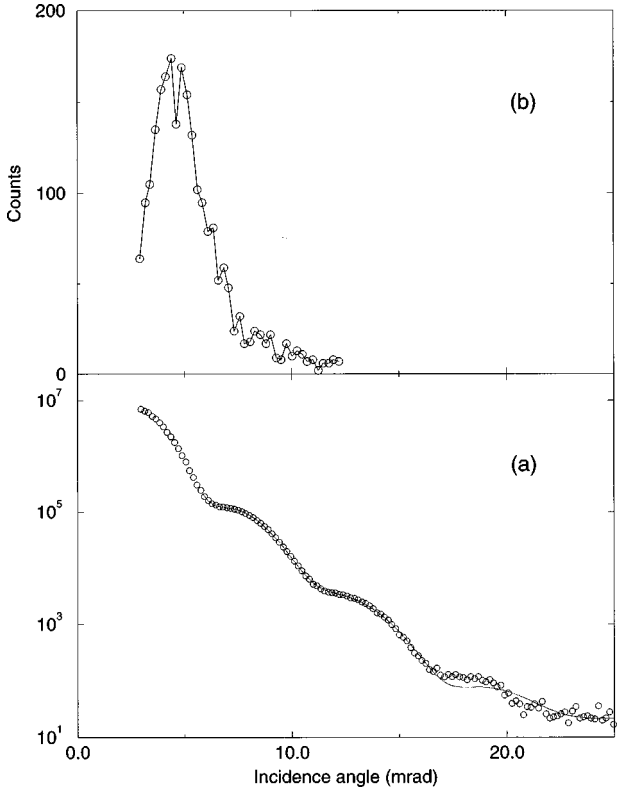

FIG. 1. (a) $\Theta-2\Theta$ scan of the specular reflected intensity of 14 403 eV synchrotron radiation with an energy bandwidth of 6 meV impinging on a Ge/Fe/Au layer (sample *A*); (b) $\Theta-2\Theta$ scan of the delayed reflected intensity due to nuclear resonant scattering, under the same conditions.

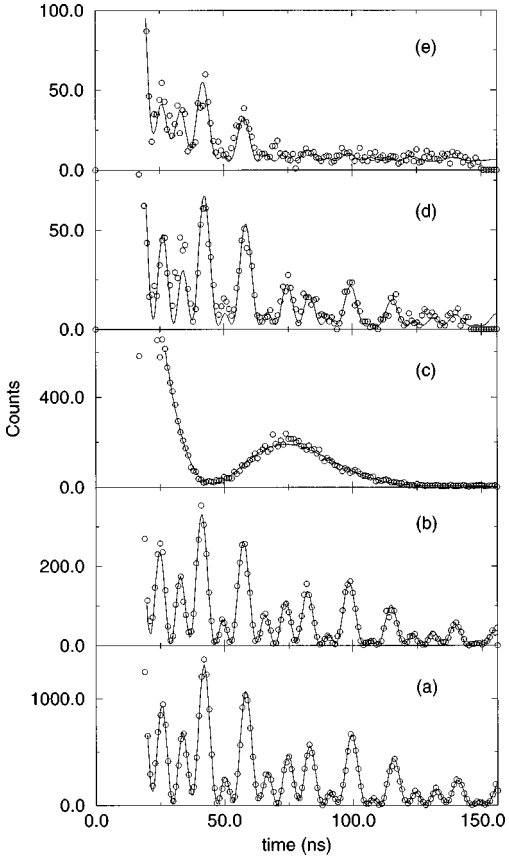

FIG. 2. Time spectra of the nuclear resonant scattering intensity under grazing incidence conditions, for five different Ge/Fe/Au layers measured at room temperature. (a) Sample *A*, $\Theta=4.7$ mrad, (b) sample *B*, $\Theta=4.7$ mrad, (c) sample *C*, $\Theta=4.7$ mrad, (d) sample *D*, $\Theta=4.0$ mrad, and (e) sample *E*, $\Theta=5.2$ mrad. The solid lines are fits using the formalism described in the text.

a fit using a standard optical formalism, with the thickness of the layers and the roughness of the interfaces as parameters. The thickness of the Fe and Au layer turned out to be 6.3(1) nm and 1.8(1) nm, respectively, while the interface roughness was taken to be Gaussian with a FWHM of 0.65(10) nm (Ge/Fe and Fe/Au) and 1.2(2) nm (Au/air). For sample *B* we obtained a Fe thickness of 6.7(1) nm, a Au thickness of 1.7(1) nm, while the roughnesses were 0.68(10), 0.74(10), and 1.4(2) nm for the Ge/Fe, the Fe/Au and the Au/air interface, respectively. This means that in both samples the Fe layer is roughly 20% thinner than expected on the basis of the growth data. The fits are insensitive to the thickness of a Ge/Fe interlayer (see later), because the refractive indices for FeGe and Fe are nearly equal. Thus, only the sum of the thicknesses of the Fe/Ge and Fe layers can be determined. It should be noted that the roughness parameter measures the uncertainty in the vertical position of the interface over a lateral range from typically 10^{-10} to 10^{-6} m. The rather large values are therefore not incompatible with the expected layer-by layer growth on terraces with a typical length of 10 nm. Figure 1(b) shows the delayed rocking curve (measured with the full beam), which has a maximum at the angle where the electronic reflectivity has the steepest slope. This is the point where the nuclear contribution to the refractive index has the largest influence on the frequency spectrum of the total reflectivity of the multilayer.[16] The decrease at lower angles is also caused by the fact that the projection of the beam becomes larger than the sample size.

For samples *A* and *B* time spectra of the delayed reflected intensity were obtained for various rocking angles between 3.4 and 9.9 mrad. The spectra at $\Theta=4.7$ mrad for samples *A* and *B* are displayed in Figs. 2(a) and 2(b). The spectra at other incidence angles are only slightly different. They are typical for a magnetic hyperfine interaction. As explained earlier, the beat pattern originates from the interference between the four simultaneously excited $\Delta m=\pm 1$ transitions. The solid curves in Fig. 2 are based on a calculation using the theory described in Sec. III. The structural parameters were taken from the rocking curve fit. It turned out that in the case of 10 ML thick probe layers the results are only moderately sensitive to the geometry of the scatterers, whereas for thinner layers the spectroscopic information is nearly completely decoupled from the structural aspects of the layer. Adjustable parameters are the vertical scale, the background and the hyperfine interaction parameters determining the complex scattering amplitude. Although a fit with one magnetic component yields already a reasonable result, a quite significant improvement is achieved by allowing for a second, nonmagnetic, component with a random orientation of the electric field gradient. This was done by assuming that the scattering amplitudes of the ^{57}Fe nuclei in different surroundings could be added coherently. We will discuss the validity of this assumption later on.

The magnetic hyperfine fields (corrected for the external field) are 32.95(3) T for sample *A* and 32.99(3) T for sample

B, not significantly different from the bulk value at 295 K. The (inhomogeneous) linewidth of the magnetic component is only $1.30(5)\Gamma_0$, where Γ_0 is the natural width of the excited state (0.097 mm/s in Doppler velocity units). This suggests a probe layer with a good structural quality. The relative intensity of the nonmagnetic component is 6(1)% for both samples. Also the hyperfine parameters were similar for both samples, with a quadrupole coupling constant $eQV_{zz}/h = 20(2)$ MHz (quadrupole splitting 0.86 mm/s) and an isomer shift $\delta = +5.8(4)$ MHz $[+0.50(4)$ mm/s] versus the magnetic component. The fit yield lines of natural width but the error is large, $\approx 0.6\Gamma_0$.

In contrast to the thicker Fe layers, the spectrum of sample *C* showed no magnetic oscillations [Fig. 2(c)]. It could be fitted reasonably well with a combination of two quadrupole components with roughly equal intensities, with $eQV_{zz}/h = 13.2(6)$ MHz and 25.5(1.0) MHz, respectively. This corresponds to quadrupole splittings of 0.57 and 1.10 mm/s. The isomer shift between the two components is <0.1 MHz and the linewidths are similar, $\Gamma = 2.4(6)\Gamma_0$. We note that the average quadrupole coupling is very close to that found for the quadrupole component in samples *A* and *B*, suggesting a common origin.

In order to check the results of this spectroscopic technique we performed CEMS experiments on samples *A*, *B*, and *C* by placing them at the cathode of a parallel-plate avalanche detector.[17] The results are shown in Fig. 3. Sample *C* is indeed nonmagnetic. The two dominant quadrupole doublets have splittings of 0.65 and 1.15 mm/s, respectively, and the same isomer shift of 0.36 mm/s versus Fe. In addition we observe a third doublet with splitting 2.3(2) mm/s, isomer shift 1.05(8) mm/s, and 10% relative intensity. The latter component was absent in the time spectra, but for the rest the results agree nicely. For the two thickest samples we see a dominant magnetic interaction with $B_{hf} = 32.95(5)$ T. In addition a quadrupole doublet is observed with $\delta = 0.36(1)$ mm/s vs Fe and a splitting of 0.86(2) mm/s (sample *A*) or 0.98(3) mm/s (sample *B*). Its relative intensity is 38(1)% for sample *A* and 23(1)% for sample *B*. The splitting is in reasonable agreement with the analysis of the time spectra but the isomer shift is definitely lower. Moreover, the relative intensity is up to a factor 4 higher than found from the time spectra.

It turns out that the puzzling differences between the NRS data and the CEMS data can be ascribed to the fact that the layers are not stable when stored at room temperature in a dry box. Whereas the NRS measurements were performed 3–4 days after the production of the samples, the CEMS data shown in Fig. 3 were obtained four months later. Subsequent CEMS measurements another three months later showed a clear increase in the nonmagnetic fraction, which now was 43(1)% for sample *A* and 30.5(5)% for sample *B*. Furthermore, the surprising third component observed before by CEMS in sample *C* was absent in this case.

In view of the results on the first three samples we decided to grow samples *D* and *E* with 1 ML thick probe layers at a distance of at least 10 ML from the Fe/Ge interface. Moreover, we did not employ *S*-passivated surfaces because the sulphur atoms may end up at the Fe/Au interface. The substrates were long (45 mm) in order to use the grazing-incidence beam as effectively as possible and thick (6 mm)

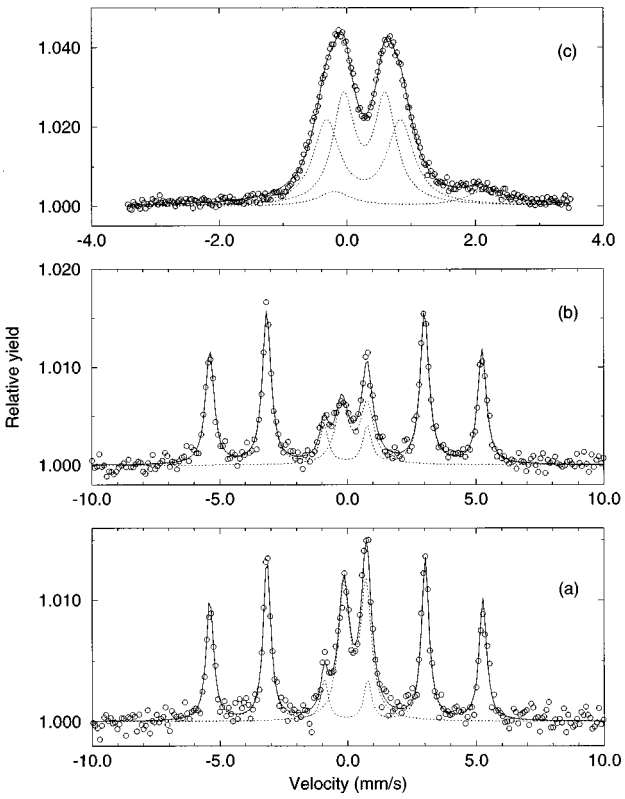

FIG. 3. Conversion electron Mössbauer spectra of three Ge/Fe/Au samples, measured at room temperature, using a source of ^{57}Co in Rh. (a) Sample *A*, (b) sample *B*, and (c) sample *C*.

to avoid complications due to substrate curvature. These samples were placed horizontally on a special Cu tailpiece of a closed-cycle refrigerator. Thermal contact was made with crycon grease. Figures 2(d) and 2(e) display the results on both samples at room temperature. The fits assume that the large majority of the ^{57}Fe nuclei experience a magnetic interaction, with average hyperfine fields of 33.00(15) T for sample *D* and 32.8(3) T for sample *E*. The linewidths are $3.4(5)\Gamma_0$ and $5.5(1.5)\Gamma_0$, respectively, much larger than in samples *A* and *B*. This points to a distribution of hyperfine fields. Such a distribution would imply different widths for different frequency components (see Ref. 25 for a recent discussion of hyperfine field distributions in NRS). However, the data are not sensitive to such a refinement. We could obtain slightly better fits by allowing for a nonmagnetic component with roughly 10% intensity for sample *D* and 20% intensity for sample *E*. Although the parameters of this component were badly defined, it was definitely not the nonmagnetic component observed in the samples *A*–*C*. For sample *D* we had a count rate of 0.4 cps, whereas it was only 0.07 cps for sample *E*. This explains the relatively poor quality of the data in Fig. 2(e), an analysis in terms of different hyperfine fields at the interface was clearly not possible. For sample *D*, a measurement at 80 K yielded $B_{hf} = 33.6(2)$ T, slightly but not significantly lower than the bulk value of 33.8 T.

V. DISCUSSION

The most puzzling observation in the measurements described here is the presence of a nonmagnetic component in

the ^{57}Fe probe layers. There is only one sensible explanation: we see interdiffusion of Ge and Fe to such an extent that each Fe in the probe layer of sample *C* is surrounded predominantly by Ge atoms. Literature values for δ in crystalline FeGe compounds are $+0.48$ mm/s for the cubic *B*20 phase[18] and about $+0.30$ mm/s for the hexagonal and monoclinic phases.[19] Only the cubic compound is not ordered at 295 K. Amorphous Fe/Ge layers are also nonmagnetic at this temperature, showing an isomer shift of 0.35–0.40 mm/s and a quadrupole splitting ranging from 0.5 to 0.9 mm/s.[20,21] These values are sufficiently close to those measured here to conclude that we have indeed a Ge/Fe interlayer of at least 9 ML thick. This result contradicts the claim of Anderson *et al.*[8] that *S*-passivation prevents intermixing. We will present a detailed comparison with the data from those authors later on.

We observe a similar nonmagnetic component in the NRS experiments on samples *A* and *B*, although only with 6% relative intensity. At this point we have a problem, because a correct analysis requires knowledge about the position of the nonmagnetic phase with respect to the Fe layer. If we assume that this component is due to an Ge-Fe interlayer with a homogeneous thickness, this layer would include the beginning of the ^{57}Fe probe layer, because a fit using such a model shows that the ^{57}Fe atoms in a 40 ML thick Ge-Fe interlayer with natural Fe contribute only 4% to the intensity of the nonmagnetic component, whereas the relative intensity of the nonmagnetic component in the probe layer is 3.5%. (Because the deeper layers are less illuminated by the photon beam than the probe layer, the fraction of 7.5% nonmagnetic ^{57}Fe atoms yields a relative intensity of only 6% in the spectrum.) However, there are two reasons to rule out such a thick homogeneous interlayer. First, from the reflectivity data of Fig. 1 it was deduced that the total thickness of FeGe+Fe is only $\approx$6.5 nm. This is already smaller than expected on the basis of the growth data if this layer is pure Fe; if the layer would be largely GeFe the discrepancy would be unacceptably large. Secondly, fits of the time spectra assuming such a thick Ge-Fe interlayer are clearly worse than those assuming a natural Fe layer of equal thickness, positioning the nonmagnetic component in or close to the probe layer. We think, therefore, that the thickness of the intermixed layer is varying locally, in some places reaching the ^{57}Fe probe layer.

For samples *A* and *B*, the combined NRS and CEMS results clearly show a progress in the Ge/Fe interdiffusion as a function of time. We also have an indication that interdiffusion took place after sample C was produced, because this sample showed a clear magnetic Kerr signal right after deposition, but no magnetic signal in the ^{57}Fe probe layer during the NRS measurements three days later. It is highly improbable that the magnetic Kerr signal originated only from the 2 ML natural Fe covering the probe layer. The increase of the intensity of the GeFe component in samples *A* and *B* is correlated with a decrease of the isomer shift. The isomer shift in the NRS data is consistent with the formation of crystalline cubic GeFe, whereas the isomer shift in the CEMS data points to the existence of an amorphous GeFe phase. We have no explanation for this puzzling behavior, nor for the fact that the interdiffusion on a long time scale (months) is more severe for sample *A* (deposited at 200 °C) than for sample *B* (produced at room temperature).

At this point we want to make a comparison with the data of Anderson *et al.*,[8] who claim that the Ge/Fe interface is sharp after deposition of Fe on a *S*-passivated Ge(100) substrate. Although we disagree on this conclusion, their experimental data are not necessarily in conflict with ours. The claim is based on Auger intensities of the various elements during deposition as a function of the thickness of the Fe layer. Due to the limited depth resolution of this method, an interdiffusion over a depth of $\approx$5 ML or less cannot be excluded. The second point is that we observe interdiffusion in a time interval of days to months, whereas Anderson *et al.* probe the profile *in situ* during deposition. Obviously, the interdiffusion on a long time scale, observed here *ex situ* in Au-capped Fe layers, is relevant for possible applications of Fe/Au multilayers grown on Ge substrates.

A complication may arise in the interpretation of NRS measurements on thin probe layers, because the assumption that one may add the contribution of the two phases coherently is not necessarily correct. Analysis of the coherence properties of the synchrotron beam has shown that although the longitudinal coherence length is very long, the effective transverse coherence length is not.[22] For the present geometry, in which the solid angle of the detector+slit is relatively large, we estimate a vertical coherence length of only 4 nm and a horizontal coherence length one order of magnitude smaller. (With a typical incidence angle of 4 mrad, the coherence length projected onto the surface is ≈ 1 μm.) This means that one should add the contribution of the two phases coherently only if a $\approx$4 nm wide section of the beam crosses both of them. For those sections where the interlayer is so thick that it reaches the probe layer this is not necessarily the case. Adding the two contributions noncoherently leads to a different picture, in which the information about the relative isomer shift is lost. However, it turns out that our NRS data cannot be fitted satisfactorily in this noncoherent picture. Whereas χ^2 decreases with roughly a factor of 2 if we add the complex nuclear scattering amplitudes of the two components, χ^2 only increases if a nonmagnetic GeFe time spectrum is simply added to a pure Fe time spectrum. We conclude that the regions in which the nonmagnetic layer reaches the ^{57}Fe probe atoms have lateral dimensions smaller than ≈ 1 μm.

Samples *D* and *E*, which were grown on nonpassivated Ge surfaces, do not show indications for the formation of an FeGe interlayer. Since the natural Fe buffer layer is only 10 ML for sample *D*, this suggests that *S*-passivation favors the interdiffusion process. On the other hand, the large linewidth for sample *D* points to a lower structural quality of the evaporated layer than in the case of samples *A*–*C*. This is in agreement with other reports concerning the growth of Fe on Ge(100).[8,23] Apparently the sulphur atoms on the surface act as surfactants, i.e., they promote two-dimensional growth of the Fe overlayer. In the absence of *S* atoms, the initial growth is in the form of three-dimensional Fe islands. The coalescence of these islands gives rise to many structural defects.

Unfortunately, an increase in linewidth directly leads to an increase of the damping of the NRS signal and an accompanying decrease of the time integral of the delayed counts. When comparing the total delayed count rate of sample *D*

with samples *A* and *B*, we also have to consider the fact that the NRS signal for these thin samples is roughly proportional to the *square* of the total number of resonant scatterers, because we sum the amplitudes of the individual contributions rather than the intensities. These two effects explain the big decrease in the total delayed count rate of samples *D* and *E*, although these samples are much bigger than samples $A-C$. The NRS spectrum of 1 monolayer of ^{57}Fe is still easily observable, but a detailed analysis is difficult. Nevertheless the results on sample *D* are surprising when compared to those on Fe/Ag(100),[2,3] where it was observed that the room temperature hyperfine field in the interior of the layer is appreciably lower than in the bulk for Fe layers thinner than $\approx$40 ML. This is attributed to a change in the spin wave spectrum. For 15 ML we expect a decrease of 0.3 T with respect to the bulk value. We do not observe this behavior, but in view of the large linewidth we cannot draw definite conclusions. The average field at the interface (sample *E*) is also higher than in the case of Fe/Ag(100). Unfortunately, the statistics of the NRS spectrum on this sample prohibit an analysis in terms of several ^{57}Fe probe atom sites at the interface.

VI. CONCLUSIONS AND OUTLOOK

The data on Ge/Fe/Au(100) structures presented here show that nuclear resonant scattering (NRS) can provide detailed information about the magnetic and structural properties of thin Fe layers. The samples showed a number of surprising features, most of which are related to the formation of a nonmagnetic GeFe interlayer. The current sensitivity limit of the method (determined by counting rate) is $\approx$1 ML. Because the signal is quadratic if the scatterers respond in phase, one can get good-quality spectra already from $\approx$3 interfaces (each 1 ML thick) in a thin multilayered sample. By taking more layers, one could even study submonolayer amounts of ^{57}Fe at the interfaces.

With the present incident photon flux, the NRS technique applied to thin layers has a sensitivity that is comparable to CEMS. Already now it is worthwhile to perform this type of NRS experiments in case one wants to measure in large magnetic fields and at various temperatures, a situation in which CEMS is difficult to apply. Although this feature is not explored here, the NRS technique is also promising for determining the direction of magnetic moments in a probe layer, especially when combined with a polarization analyzer behind the sample.[24]

ACKNOWLEDGMENTS

The authors would like to thank C. R. Laurens and F. C. Voogt for help during the measurements. They also thank the ESRF staff, in particular J. Ejton and Z. Hubert, for providing the excellent conditions which made these experiments possible.

*Present address: CEIT, Departamento de Materiale, 200009 San Sebastian, Spain.

†Present address: SPring8/JASRI, Kamigoro-cho, Ako Gun, Hyogo 678-12, Japan.

[1] For a recent review, see, e.g., *Ultrathin Magnetic Structures*, edited by J. A. C. Bland and B. Heinrich (Springer, Berlin, 1994), Vols. 1 and 2.

[2] G. Liu and U. Gradmann, J. Magn. Magn. Mater. **118**, 99 (1993).

[3] P. J. Schurer, Z. Celinski, and B. Heinrich, Phys. Rev. B **48**, 2577 (1993); **51**, 2506 (1995).

[4] R. Rüffer and A. Chumakov, Hyperfine Interact. **97/98**, 589 (1996).

[5] A. I. Chumakov, G. V. Smirnov, A. Q. R. Baron, J. Arthur, D. E. Brown, S. L. Ruby, G. S. Brown, and N. N. Salashchenko, Phys. Rev. Lett. **71**, 2489 (1993).

[6] T. S. Toellner, W. Sturhahn, R. Röhlsberger, E. E. Alp, C. H. Sowers, and E. E. Fullerton, Phys. Rev. Lett. **74**, 3475 (1995).

[7] W. Folkerts, W. Hoving, and W. Coene, J. Appl. Phys. **71**, 362 (1992).

[8] G. W. Anderson, P. Ma, and P. R. Norton, J. Appl. Phys. **79**, 5641 (1996).

[9] K. Shintaku, Y. Daitoh, and T. Shinjo, Phys. Rev. B **47**, 14 584 (1993).

[10] A. Q. R. Baron, Nucl. Instrum. Methods Phys. Res. A **353**, 665 (1994).

[11] Y. Kagan, A. M. Afanas'ev, and V. G. Kohn, J. Phys. C **12**, 615 (1979).

[12] J. P. Hannon, N. V. Hung, G. T. Trammell, E. Gerdau, M. Mueller, R. Rüffer, and H. Winkler, Phys. Rev. B **32**, 5068 (1985); J. P. Hannon, G. T. Trammell, M. Mueller, E. Gerdau, R. Rüffer, and H. Winkler, *ibid.* **32**, 6363 (1985).

[13] L. Nevot and P. Croce, Rev. Phys. Appl. **15**, 761 (1980).

[14] The computer code written for this calculation is based on A. Q. R. Baron, thesis, Stanford, 1995.

[15] H. Kiessig, Ann. Phys. (Paris) **10**, 769 (1931).

[16] A. Q. R. Baron, J. Arthur, S. L. Ruby, A. I. Chumakov, G. V. Smirnov, and G. S. Brown, Phys. Rev. B **50**, 10 354 (1994).

[17] G. Weyer, in *Mössbauer Effect Methodology*, edited by I. J. Gruverman (Plenum, New York, 1976), Vol. 10, p. 301.

[18] R. Wäppling and L. Häggström, Phys. Lett. **28A**, 173 (1968).

[19] R. Wäppling, L. Häggström, and E. Karlsson, Phys. Scr. **2**, 233 (1970).

[20] O. Massenet and H. Daver, Solid State Commun. **21**, 37 (1977).

[21] J. Patankar, Y. V. Bhandarkar, S. M. Kanetkar, S. B. Ogale, and V. G. Bhide, Nucl. Instrum. Methods Phys. Res. B **7/8**, 720 (1985).

[22] A. Q. R. Baron, A. I. Chumakov, H. F. Grünsteudel, H. Grünsteudel, L. Niesen, and R. Rüffer, Phys. Rev. Lett. **77**, 4808 (1996).

[23] G. A. Prinz, in *Ultrathin Magnetic Structures* (Ref. 1), p. 35.

[24] D. P. Siddons, U. Bergmann, and J. B. Hastings, Phys. Rev. Lett. **70**, 359 (1993).

[25] Yu. V. Shvyd'ko, U. van Bürck, W. Potzel, P. Schindelmann, E. Gerdau, O. Leupold, J. Metge, H. D. Rüter, and G. V. Smirnov, Phys. Rev. B **57**, 3552 (1998).